Charged particle multiplicities from MRS tracking detectors

F.Rami (fouad.rami@ires.in2p3.fr)
November 17, 2000

In this note, I describe briefly the status of my analysis work concerning the extraction of charged particle multiplicities from MRS tracking detectors (MTPC1 and MTPC2). The objective is to provide an estimate of dN/dη in the central region (around $\eta = 0$), to be used as complementary/redundant to the results obtained from global detectors (tiles and BB). Tracking detectors have the advantage to allow direct measurements of particle multiplicities and in addition one can easily remove "secondaries". They have however their own problems due mainly to the inefficiency of the reconstruction (clustering/tracking) procedure.

The report is organized as follows. After a brief description of the analysis procedure (section 1) and the event selection (section 2), I will give some details on the primary vertex used in the analysis (section 3). Then I will describe in section 4 how the measured multiplicities were converted into dN/dη and I will present some typical results.

1 Some details on the analysis procedure

Same tracking/clustering methods were used for both TPC's (MTPC1 and MTPC2). Clustering was done using the BrTPCCluster class with its default parameters. Track reconstruction was performed with the BrTPCTrackingModule class with the following parameters:

- SetTsigLow(1.2)
- SetTsigHigh(2.6)
- SetSearchWidthX(0.60)
- SetSearchWidthY(0.50)
- SetHitSearchWidthX(0.4)
- SetHitSearchWidthY(0.7)
- SetClusterMethod(0)
- SetTrackMethod(0)

Geometry parameters were taken from the most recent survey results (see analysis Note#8 of Sept. 24 by F.Videbaek). The .geo files used (for different angle settings) can be found in /home/rami/root−app/tpc/mrs−theta.geo. The drift velocity was taken equal to 1.6 cm/μsec. All data files considered in the present analysis are with Zero magnetic field on D5 and mainly for $\theta = 90°$ setting. Due to the small acceptance of the MRS and the narrow vertex cut used in the analysis (see below), a large number of data files (36 sequences for $\theta = 90°$-setting) was used in order to accumulate reasonable statistics for central collisions.

2 Event selection and collision centrality

In the present analysis, only "trigger 6" events were considered. To classify those events according to their degree of centrality, I have used the sum ADC distribution extracted from the tiles.

Fig.1 shows the multiplicity (1 MIP equivalent) distribution of charged particles in the tiles. An arbitrary normalization was applied to define "reduced multiplicities" (the normalization method is not an important issue at the present stage of the analysis). The distribution exhibits the typical shape, well known at lower energies (AGS, SPS), with a rapid fall-off at the highest multiplicities. It is slightly different from the one obtained by JH Lee (Analysis note #14). This is due to the fact that I did'nt introduce any geometry/acceptance corrections.

To isolate the most central collisions, I used two centrality cuts defined at, respectively, 12% and 8% of the total number of events (trigger 6). The 8% cut in the present analysis corresponds roughly to a 6% (PHOBOS) cut on the minimum bias distribution (I assume that "trigger 6" represents about 75% of the minimum bias).

3 Definition of the collision primary vertex

The primary vertex of each event was extracted from beam-beam counters as the time difference between averaged times of left and right tubes. An offset of 1.5 cm was introduced to take into account the systematic shift observed between the vertices obtained from BB and tracking detectors.

Note that all analyzed events (trigger 6) have a vertex from BB counters (no need to combine BB and ZDC vertices).

Fig.2 shows the primary vertex distribution determined as described above.

In the present analysis, a narrow cut of ± 3 cm was imposed on the collision vertex. Under this cut, one can reasonably assume that all primary tracks are originating from the nominal intersection point which simplifies the procedure to extract $dN/d\eta$ (next section). The introduction of this cut reduces however significantly the statistics (only a small fraction of the available events satisfies this condition on the vertex).

Fig.3 shows examples of track multiplicities distributions reconstructed in the front TPC (MTPC1). The distribution displayed in the lower panel of this figure is obtained under the 12% centrality cut (previous section). One sees, as expected, larger particle multiplicities in central collisions. Note that the mean value of the distribution (not corrected for tracking efficiency) is relatively low with only ~ 5 tracks per central event. The effect of the vertex cut is illustrated in the mid-panel: i) there is a drastic reduction in the number of events and ii) one sees larger multiplities as expected from acceptance considerations.

Fig.4 shows the track multiplicity in both TPC's (MTPC1 and MTPC2) as a function of the collision centrality (from Fig.1). Error bars are statistical uncertainties only. The multiplicities presented in these figures include all tracks (including secondaries) reconstructed by the TPC's and they are not corrected for the tracking inefficiency. It is also important to keep in mind that these results were obtained with the tracking parameters listed in page 1. The latter parameters need still to be optimized and this might affect significantly the values of the multiplicities.

The observed trend (Fig.4) exhibits an almost linear dependence between the track multiplicity in the TPC and the global (tiles) multiplicity. This is illustrated by the solid curves obtained by fitting a second order polynomial function to the data points. Note that the statistics is very low at the highest centrality bins which makes difficult to draw any conclusion (about the linearity) in this region.

4 Extraction of the pseudo-rapidity density in the central region

To convert the measured multiplicities into dN/dη values, I assumed that all primary tracks originate from the nominal intersection point. This assumption is justified by the very narrow cut ($\pm$3 cm) imposed on the collision vertex. Then I extracted the values of dN/dη as follows:

$$dN/d\eta = Mul \times f_\Phi \times f_\eta$$

dN/dη is the pseudo-rapidity density, i.e. the number of charged particles per unit of pseudo-rapidity. Mul is the measured track multiplicity within the TPC acceptance.

f_Φ is introduced to take into account the limited azimuthal acceptance of the TPC:

$f_\Phi = 360°/\Delta\Phi$ where $\Delta\Phi$ is the azimuthal angle covered by the TPC.

$f_\eta = 1/\Delta\eta$ is a correction factor which takes into account the pseudo-rapidity coverage ($\Delta\eta$) of the TPC. $\Delta\eta$ is obtained from the polar angle $\Delta\theta$ covered by the TPC.

$\Delta\Phi$ and $\Delta\theta$ were calculated for each TPC with respect to the pad plane (row) before the last one.

The values of $\Delta\Phi$, f_Φ, $\Delta\theta$, $\Delta\eta$ and f_η are given in Table 1 in the case of the 90°-setting ($\eta = 0$).

In the future, conditions on θ and Φ will be introduced in the analysis in order to include only tracks within $\Delta\theta$ and $\Delta\Phi$. This will have as an effect to lower slightly the values of the multiplicities.

	$\Delta\Phi$ (deg.)	f_Φ	$\Delta\theta$ (deg.)	$\Delta\eta$	f_η
MTPC1	10.94	32.91	20.84	0.366	2.734
MTPC2	2.47	145.7	12.50	0.219	4.575

Table 1:

Fig.5 shows the results, expressed in terms of the pseudo-rapidity density around $\eta = 0$, as a function of the collision centrality. Here all reconstructed tracks are included (not only primary particles).

The next step was then to remove particles not originating from the primary collision vertex (i.e. secondaries). This includes mainly background tracks (+ some of the weak decays). Rejection of those secondaries has been done by looking at the projections of particle tracks towards the interaction plane. This is what is plotted in Fig.6 for both y (vertical) and z (beam axis) directions. Secondary particles appear in the tails of these distributions.

To get a first estimate of the fraction of secondary particles, I introduced some conditions on the track projections. I applied asymmetric cuts to take into account the slight asymmery observed in the distributions (see Fig.6). The limits of the cuts used in the analysis are listed in Table 2.

	cuts in y (cm)	cuts in z (cm)	fraction of secondaries
MTPC1	-7 - 6	-20 - 19	16%($*$)
MTPC2	-21 - 19	-31 - 29	19% (*)

Table 2:

(*) This number is an average number for all trigger 6 events. It is a bit larger for the most central collisions.

These cuts are larger than 3 σ. Cutting at 3 σ, the fraction of secondaries is larger by a about a factor of two than the numbers given in Table 2. It is not clear yet how to set the values of these cuts (on the basis of simulations ?).

As already mentioned, the present analysis was done using the primary vertex provided by the BB counters. It would be of course much better in future analyses to use the vertex from tracking detectors. This is possible but only in the case of highly central collisions where the number of reconstrucetd tracks is sufficient (at least 2) to define a collision vertex from the TPC.

The results obtained after rejecting secondary particles are displayed in Fig.7 in the case of the $\theta = 90°$-setting. The results for the $\theta = 60°$-setting are shown in Fig.8. I also analyzed the $\theta = 45°$-data but the statistics available for this setting was not sufficient for a fine binning on the centrality.

Fig.9 shows the values of the pseudo-rapidity density dN/dη extracted from the TPC's under the 8% centrality cut. The values at $\theta = 45°$ (points at $\eta \sim 0.9$ are also plotted in this figure but statistical errors are very large (in particular for MTPC2). Here, the results are presented for all reconstructed tracks (including secondaries).

It is interesting to notice that the extracted values (Fig.9) are not very different from those obtained from global detectors (and PHOBOS). For a quantitative comparison, one should take into account tracking inefficiency and use the same centrality cut.

Note also that the results obtained from MTPC1 and MTPC2 are consistent. MTPC2 gives slightly higher values which might be due to a difference in the tracking efficiency (MTPC1 is less efficient because of higher background and higher track density). It might be also due to the fact that the tracking program rejects events with a large number of clusters ("Number of clusters exceeds any reasonable limit"). Such events occur only in MTPC1. Whether all those events are "background" is not clear and we might reject a significant number of "true" high multiplicity events. I noticed that the fraction of these events is correlated with the centrality (higher in central collisions). This deserves to be investigated in more detail.

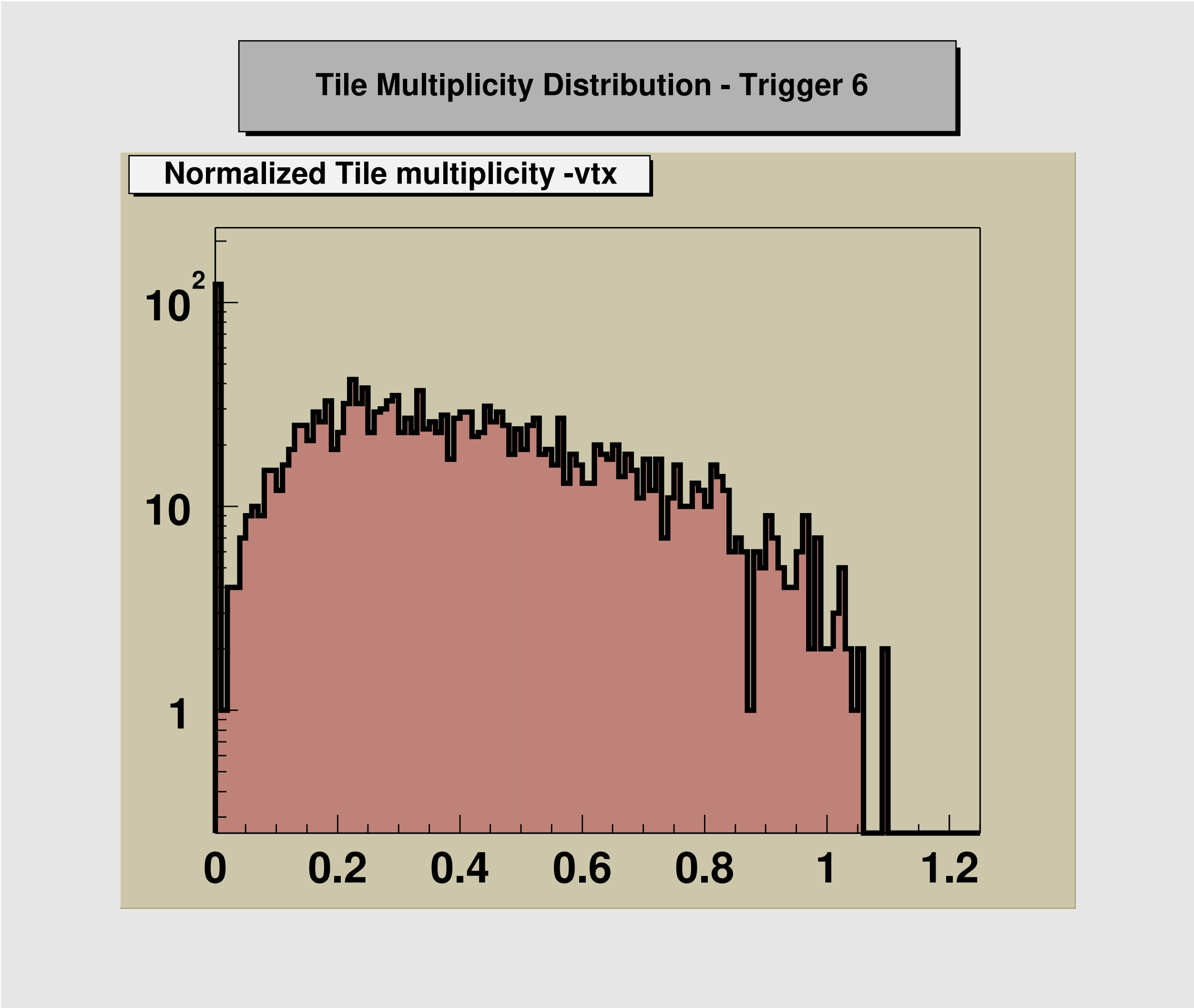

Figure 1: Multiplicity (1 MIP equivalent) distribution of charged particles in the tiles. Multiplicities are normalized to a constant value (=2650). The 12% centrality cut corresponds the multiplicity region above 0.58 in this plot.

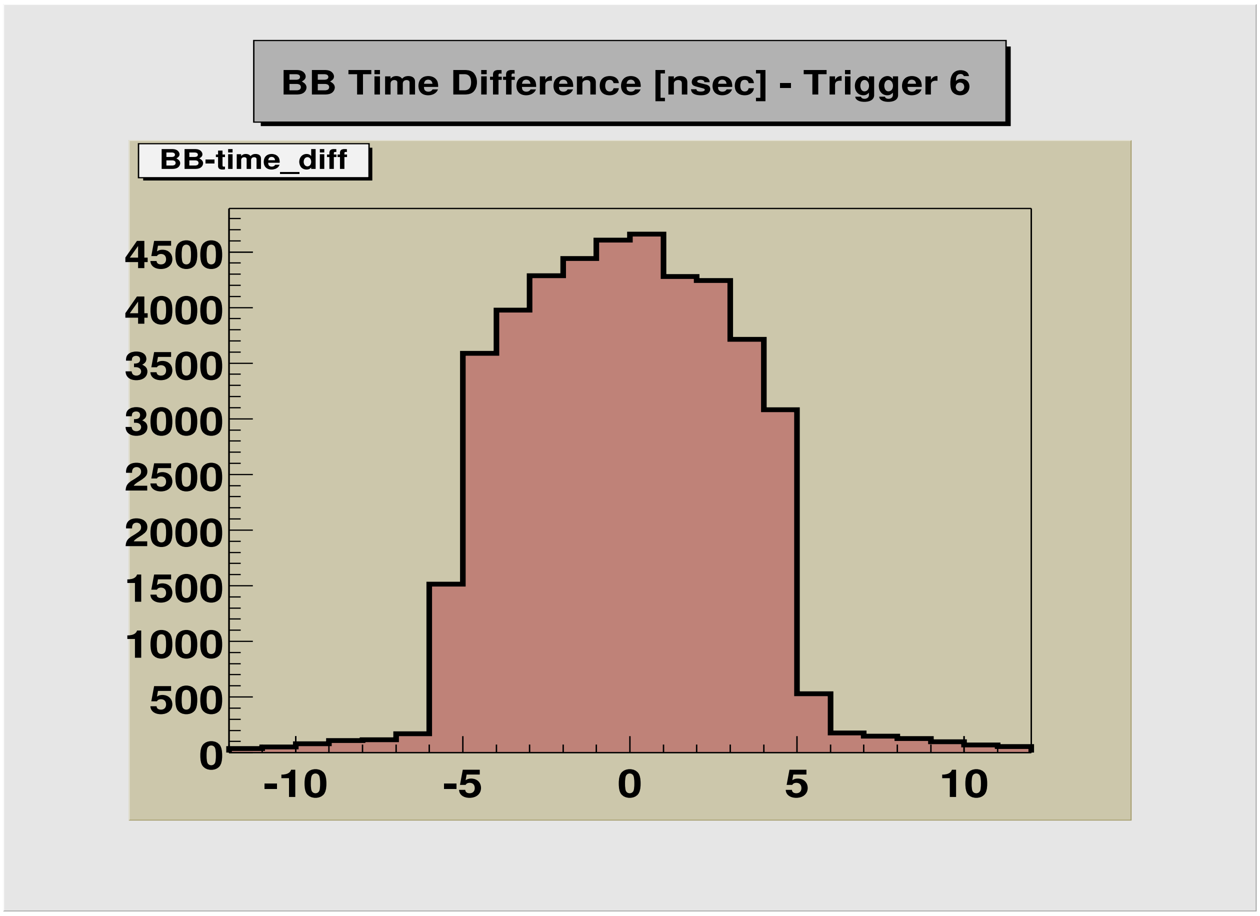

Figure 2: Beam-Beam time difference (in nsec). The ± 3 cm vertex cut (used in the present analysis) corresponds to a ± 0.2 nsec cut in this figure.

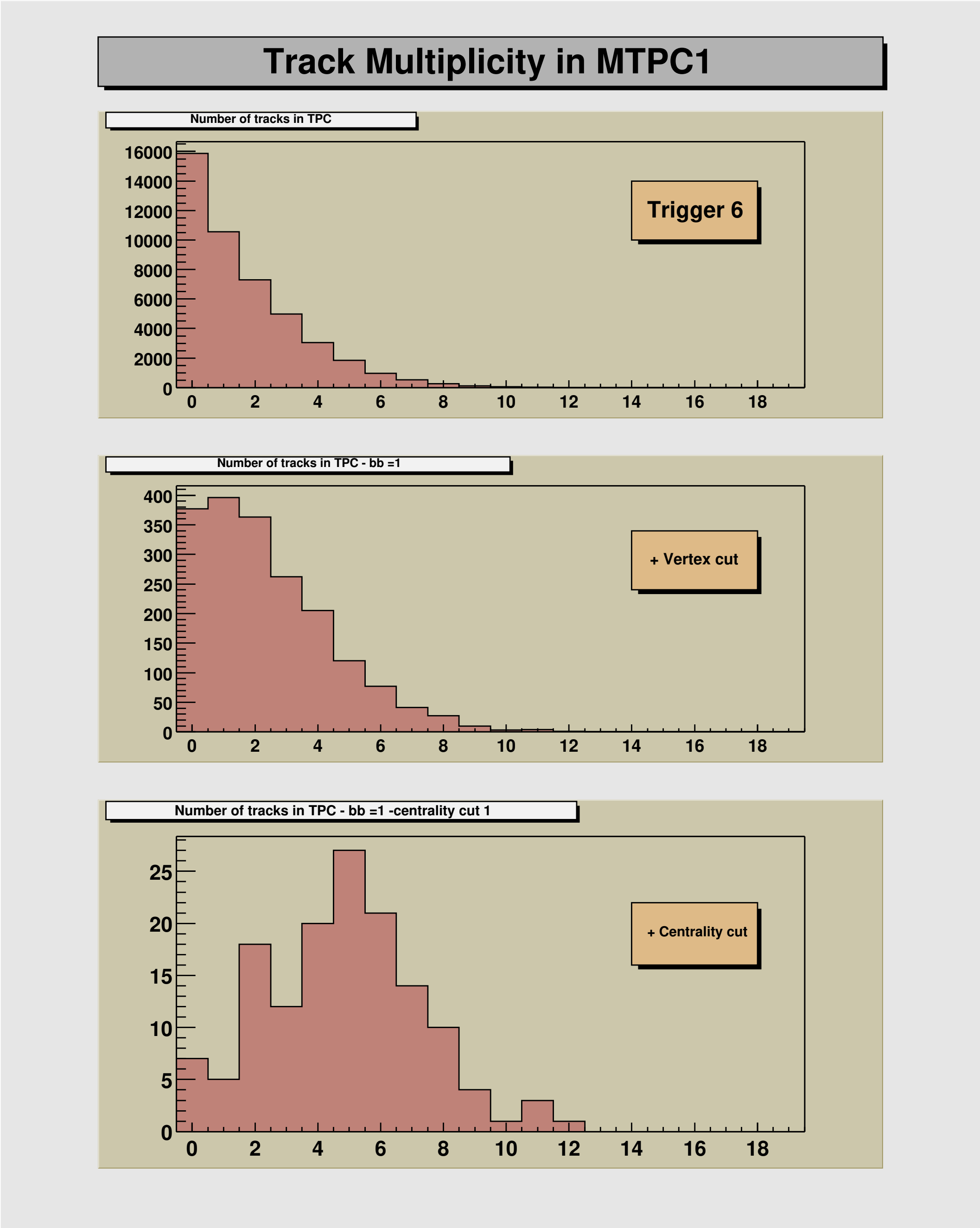

Figure 3: Track multiplicity distribution from MTPC1. Top panel: all "trigger 6" events. Mid panel: with a ± 3 cm cut on the vertex. Bottom: under the 12% centrality cut.

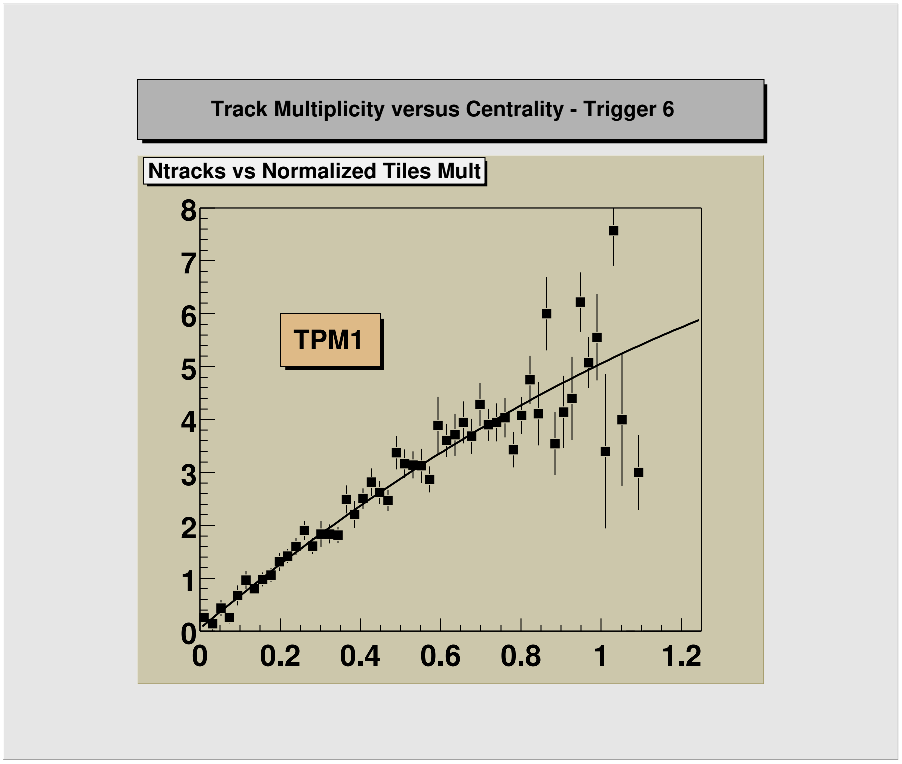

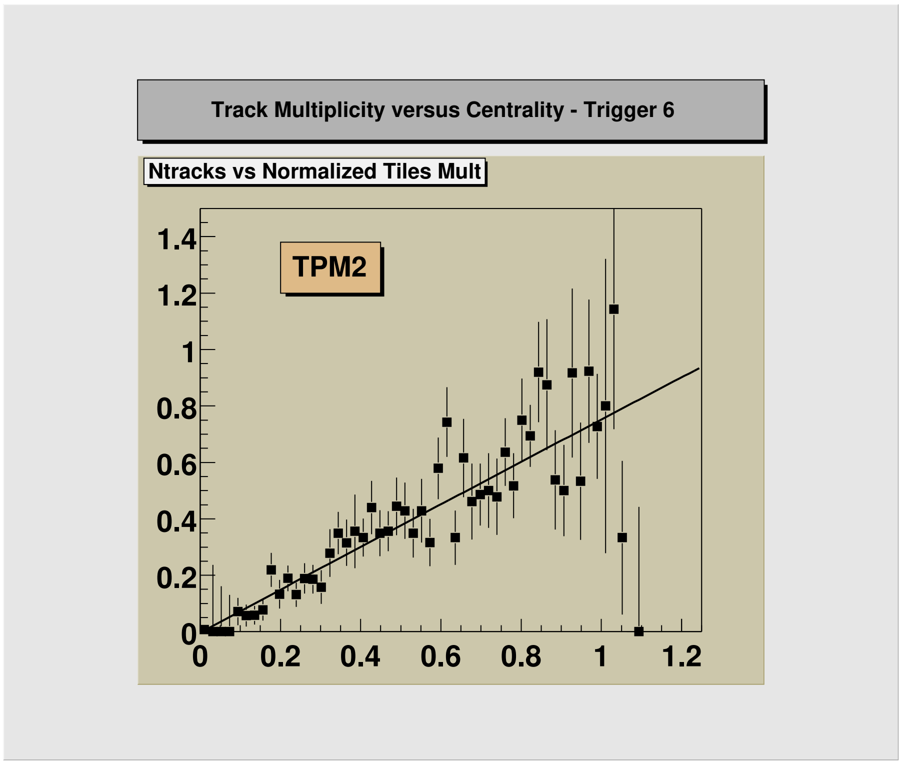

Figure 4: Track multiplicity in MTPC1 (top) and MTPC2 (bottom) as a function of the collision centrality (i.e. multiplicity in the tiles). The results are shown for the $\theta = 90°$-setting.

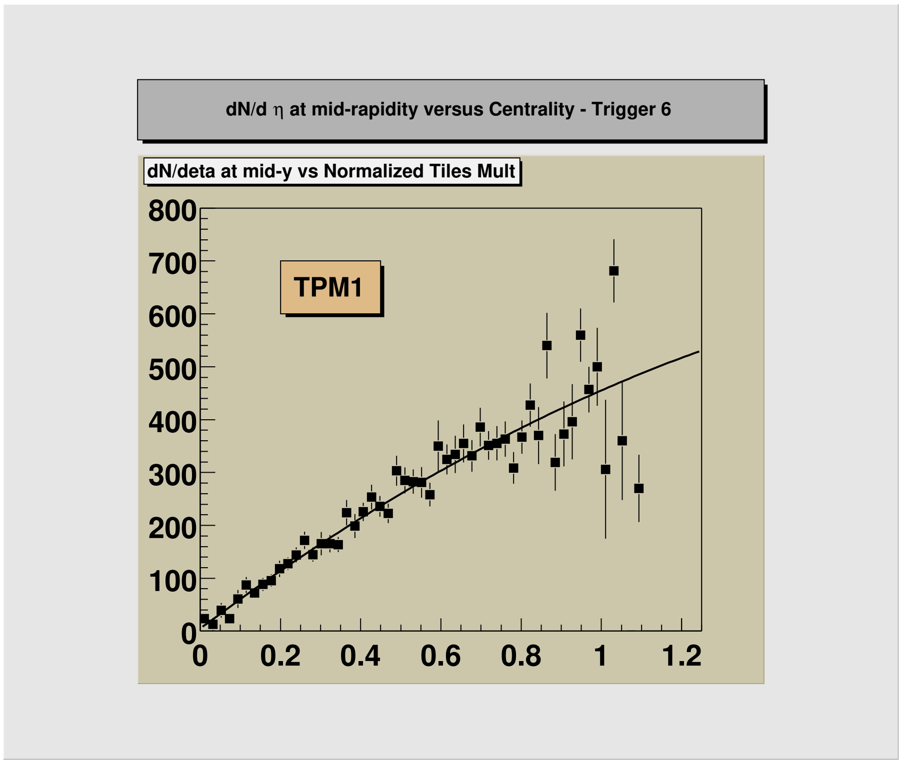

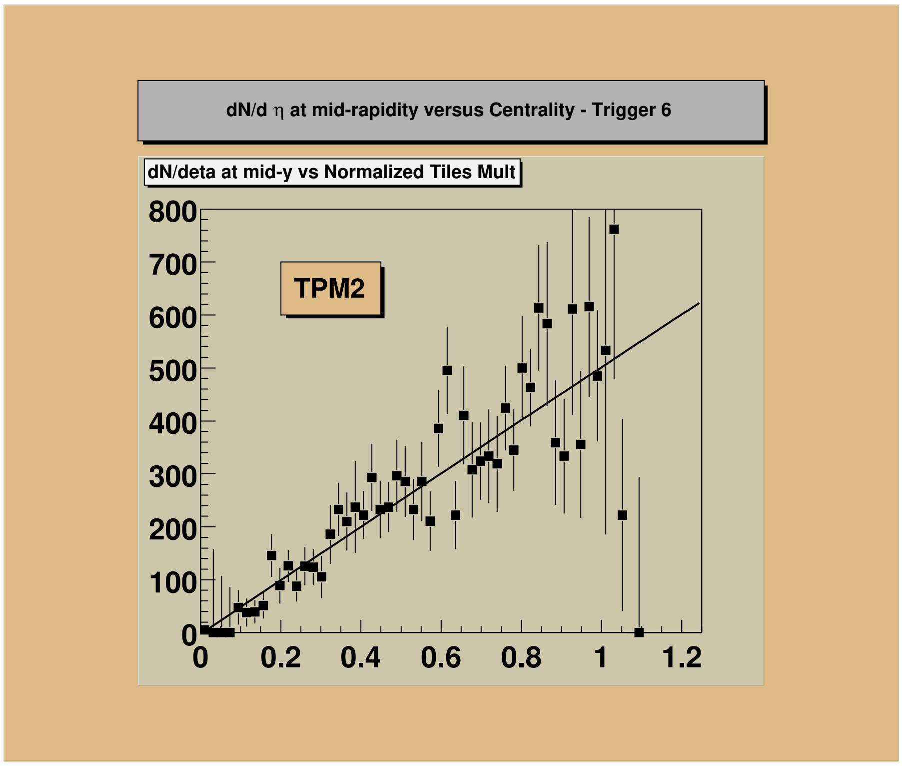

Figure 5: Pseudo-rapidity density at mid-rapidity ($\theta = 90^\circ$) as a function of the collision centrality (i.e. multiplicity in the tiles).

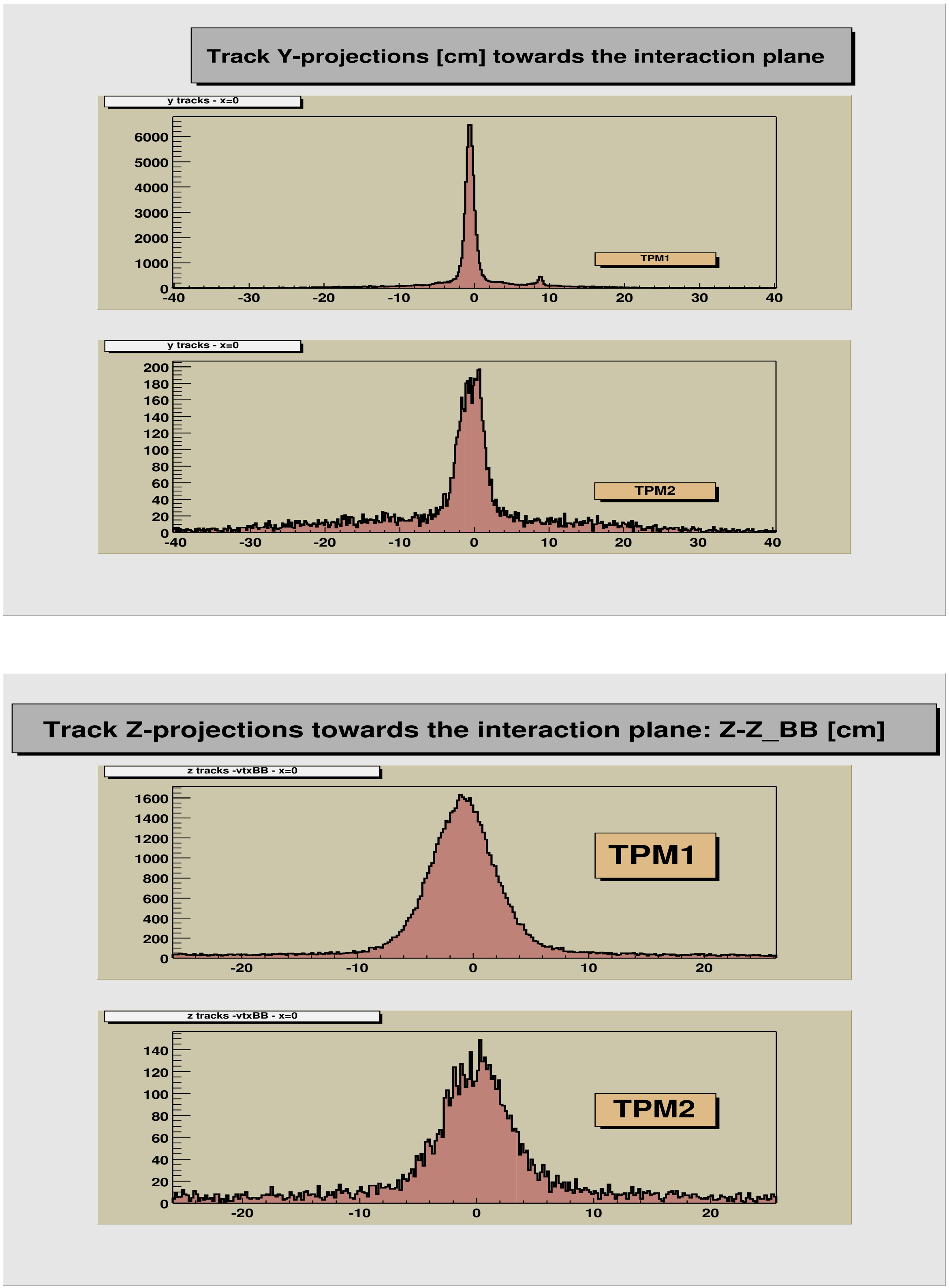

Figure 6: Track projections towards the interaction plane (top: y−projections, bottom: z−projections). The z−projection is plotted as the difference between z and the collision vertex ($z - z_{BB}$).

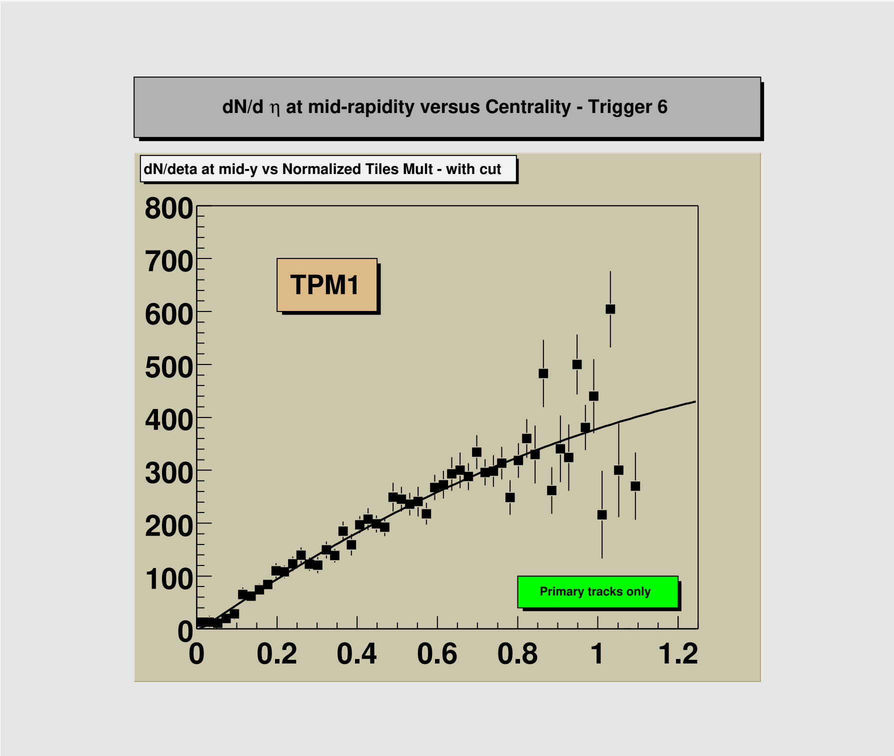

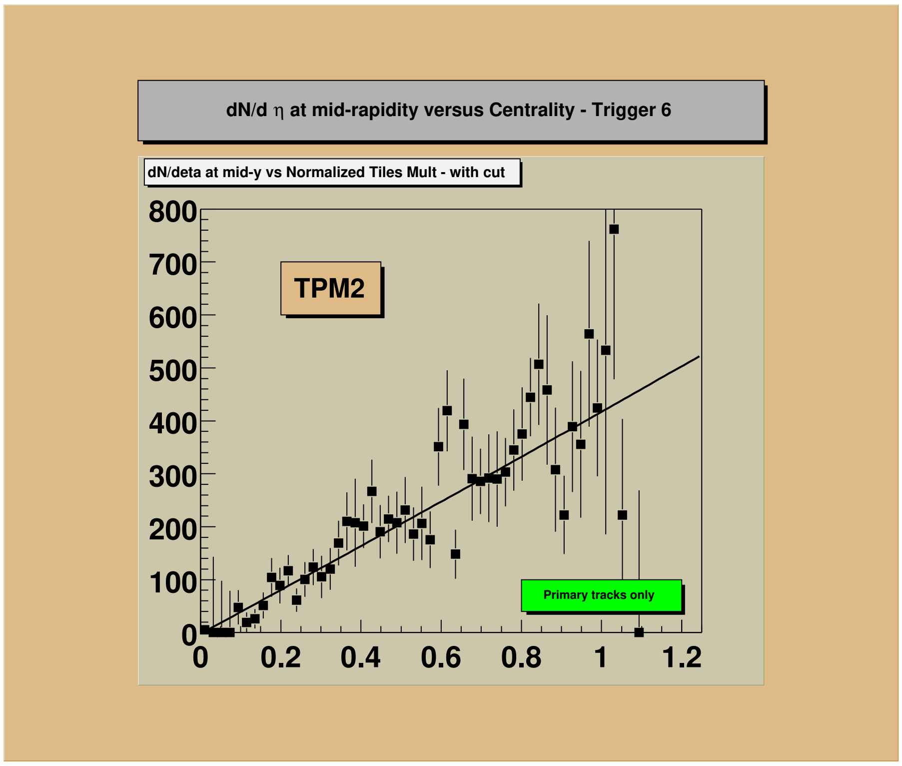

Figure 7: Pseudo-rapidity density at mid-rapidity ($\theta = 90°$) as a function of the collision centrality (i.e. multiplicity in the tiles). Here, only primary tracks are included in the multiplicities.

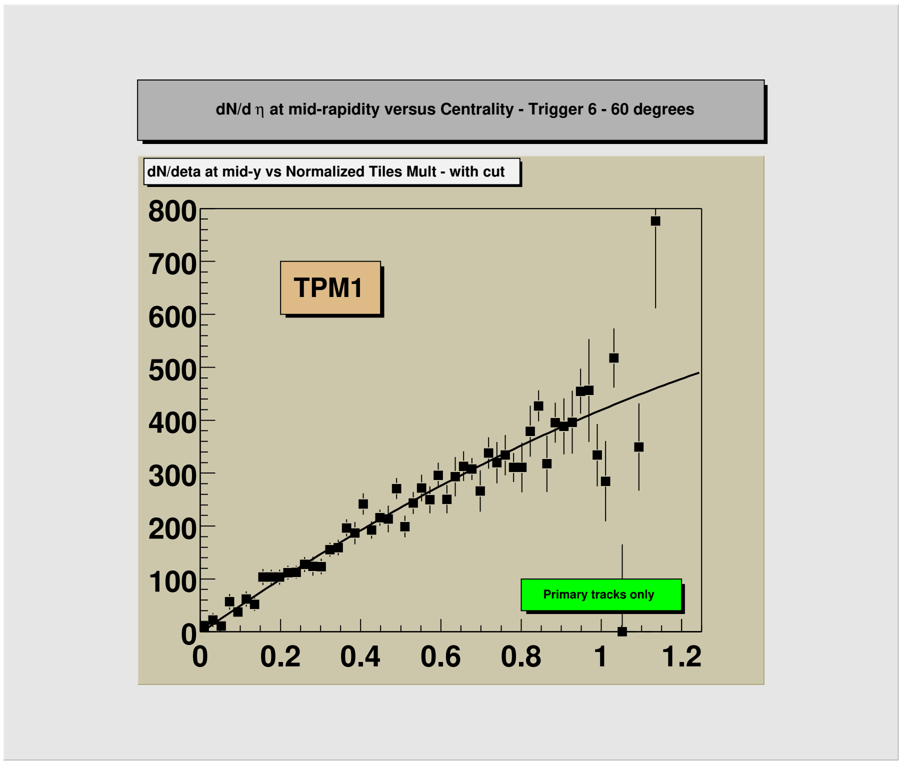

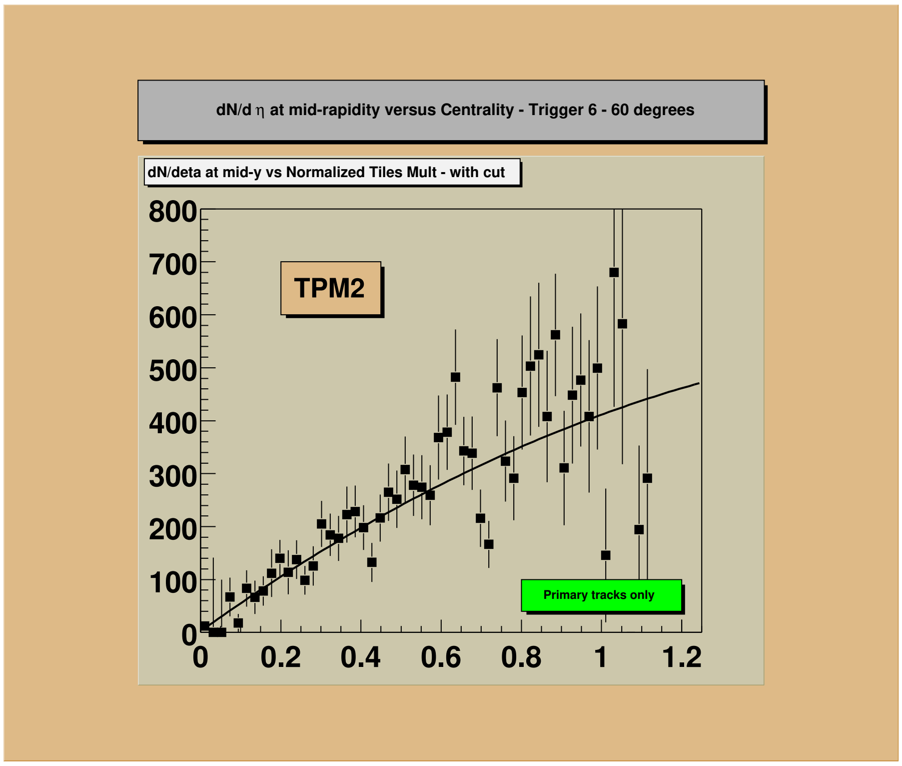

Figure 8: Same as Fig.7 for the $\theta = 60°$-setting.

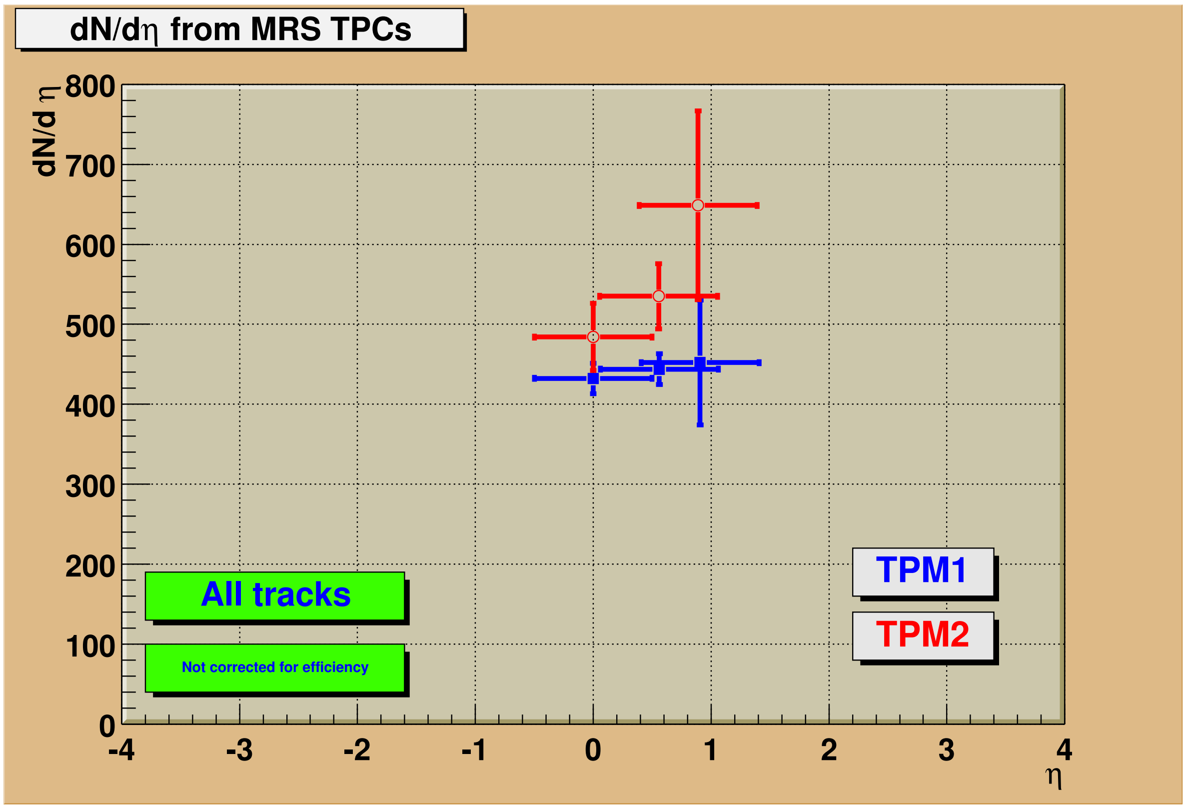

Figure 9: Pseudo-rapidity density for the three MRS settings (90, 60 and 45 degrees). The results are presented for the 8% centrality cut. Here all reconstructed tracks are included (no rejection of secondaries). Error bars are statistical uncertainties only.